Supplementary Information

Conductive dual hydrogen-bonding hydrogels for electrical stimulation of infected chronic wounds

Ye Wu[1†], Yuhui Lu[2†], Can Wu[2], Jiali Chen[1], Ning Ning[1], Zeyu Yang[3], Yi Guo[3], Jieyu Zhang[2]*, Xuefeng Hu[2]*, Yunbing Wang[2]

[1]Department of Orthopedics, Orthopedic Research Institute, West China Hospital, Sichuan University, Chengdu, Sichuan, 610041, China

[2]National Engineering Research Center for Biomaterials, Sichuan University, Chengdu, Sichuan, 610065, China

[3]Rotex Co., Ltd, D6-1104, Tianfu Software Park, High-Tech Zone, Chengdu, Sichuan, 610064, China

*Corresponding author:

29 Wang Jiang Road, Chengdu, China, 610065
Email: jieyu@scu.edu.cn; hu_xf@qq.com

†Equal contribution.

Table S1. Preparation of hydrogels with different compounds.

Sample	CS or its derivative (mg)	NAGA or AM (g)	PBS (mL)	APS (μL)	TEMED (μL)
QCSP-g-PNAGA-0.4	90 (QCSP)	0.4 (NAGA)	2.4	90	90
QCSP-g-PNAGA-0.5	90 (QCSP)	0.5 (NAGA)	2.4	120	120
QCSP-g-PNAGA-0.6	90 (QCSP)	0.6 (NAGA)	2.4	150	150
QCSP-g-PNAGA-0.7	90 (QCSP)	0.7 (NAGA)	2.4	180	180
QCS-g-PNAGA-0.6	90 (QCS)	0.6 (NAGA)	2.4	150	150
CS-g-PNAGA-0.6	90 (CS)	0.6 (NAGA)	2.4	150	150
QCSP-g-PAM-0.6	90 (QCSP)	0.6 (AM)	2.4	150	150

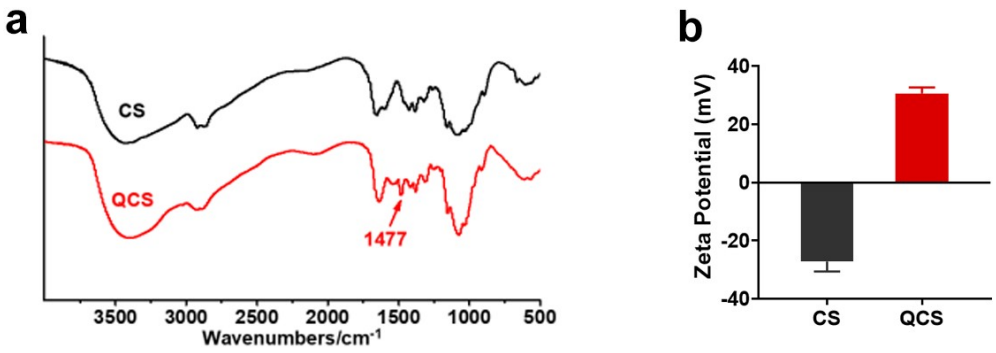

Fig. S1. FTIR spectra (a) and zeta potential (b) of CS and QCS.

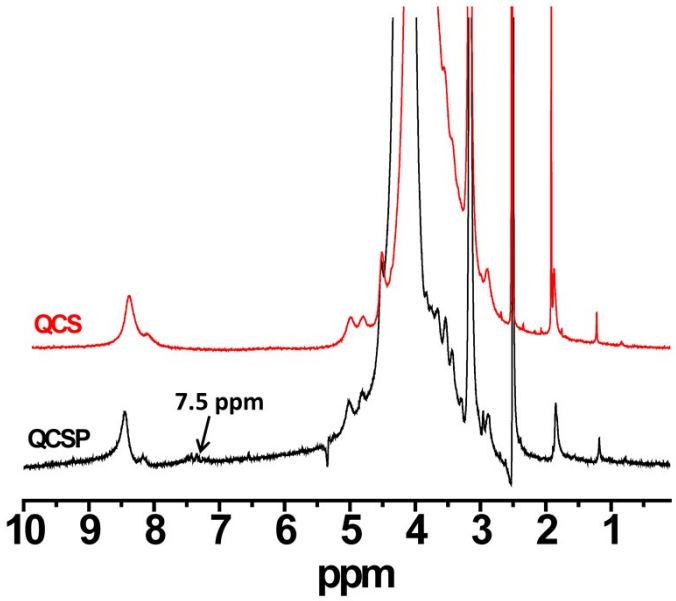

Fig. S2. ^{1}H NMR spectra of QCS and QCSP.

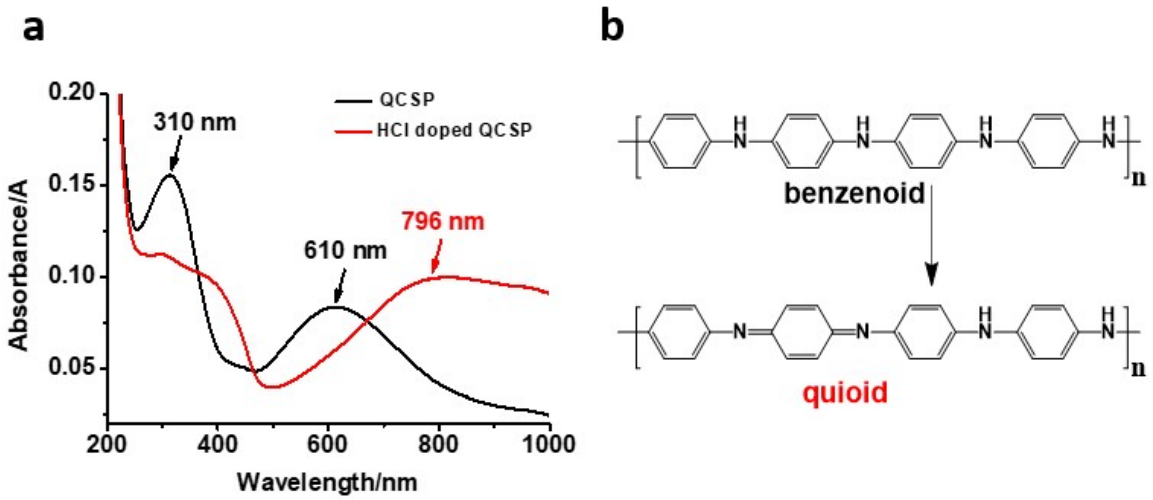

Fig. S3. (a) UV/Vis spectra of QCSP before and after doping with 1 M HCl. (b) Transition of benzenoid to quinoid of polyaniline.

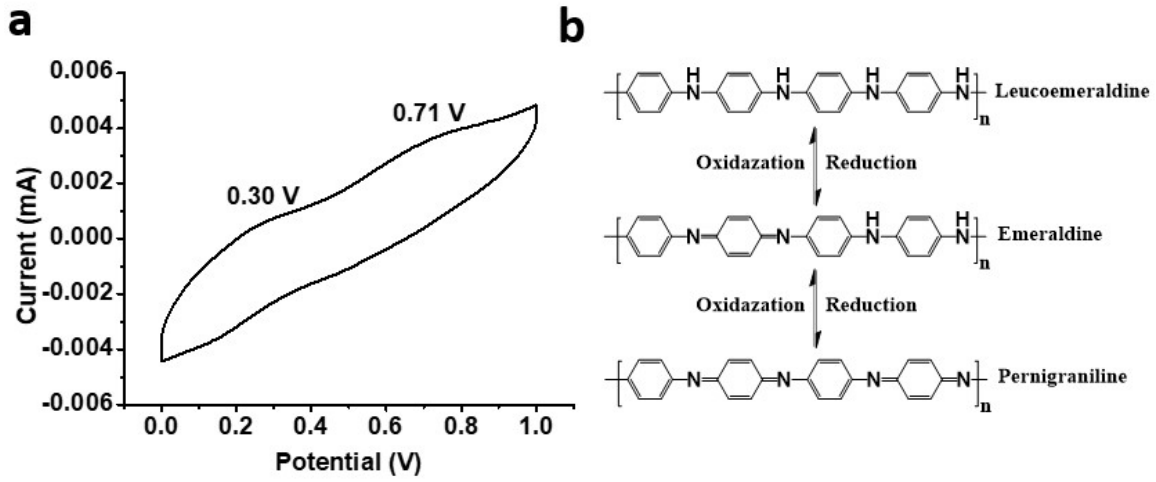

Fig. S4. (a) Cyclic voltammogram of QCSP. (b) Molecular structure of polyaniline segments in QCSP in different oxidation states.

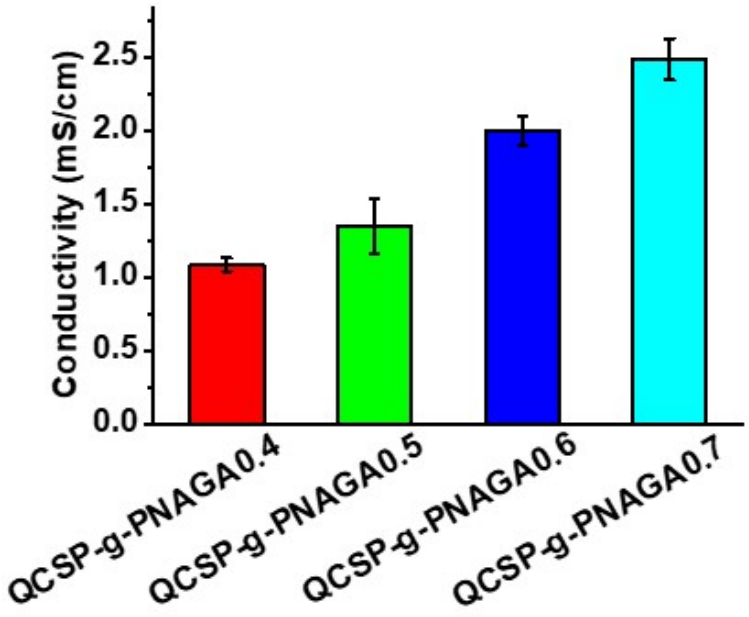

Fig. S5. Conductivity of the QCSP-g-PNAGA hydrogels with different PNAGA content.

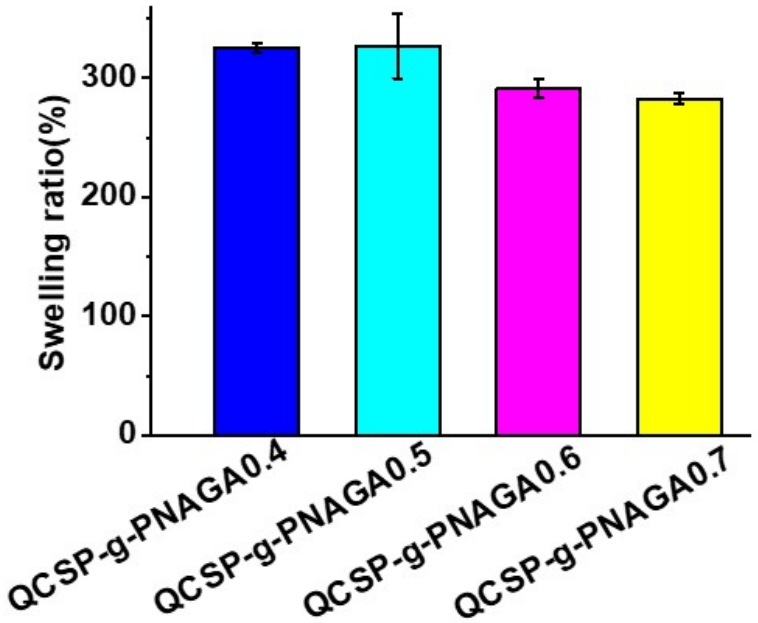

Fig. S6. Swelling ratios of the QCSP-g-PNAGA hydrogels with different PNAGA content.

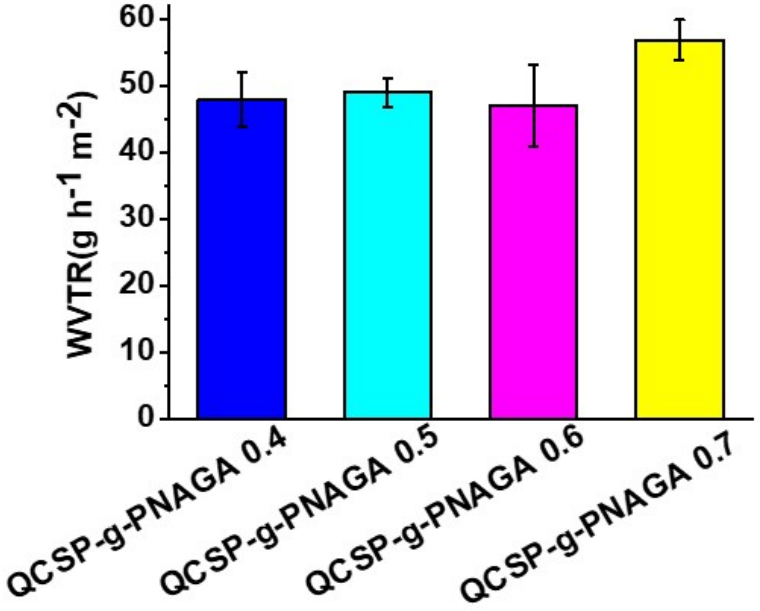

Fig. S7. WVTRs of the QCSP-g-PNAGA hydrogels with different PNAGA content.

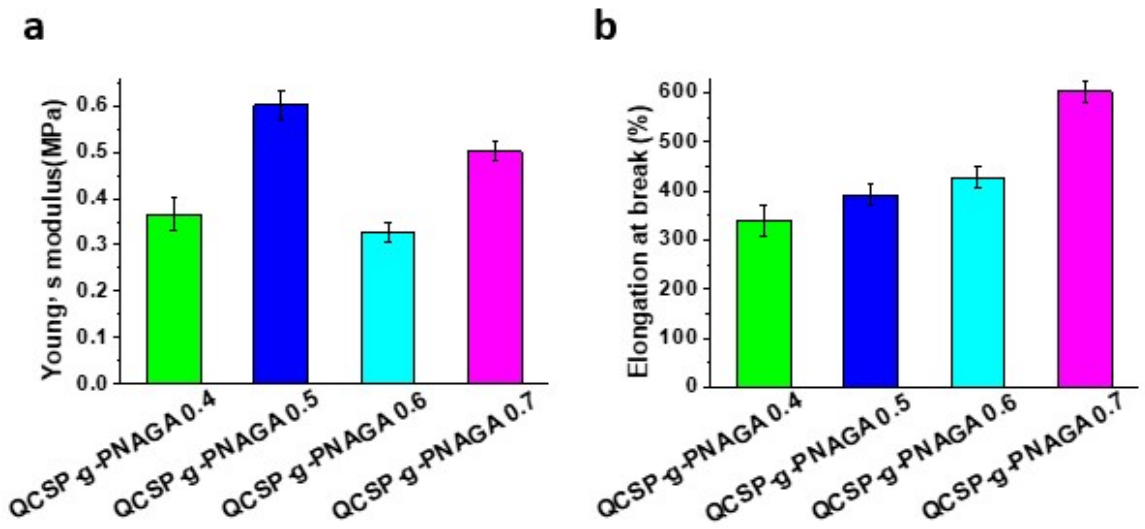

Fig. S8. Young's modulus and elongation at break of the QCSP-g-PNAGA hydrogels with different PNAGA content.

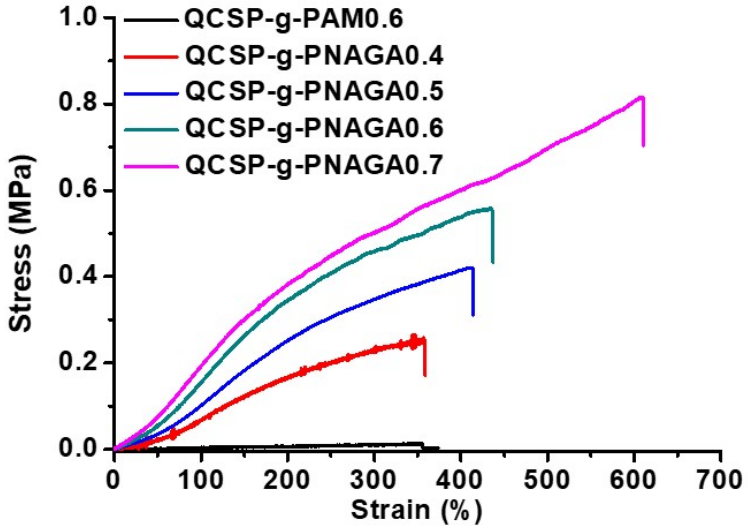

Fig. S9. Tensile stress-strain curves of the different hydrogels.

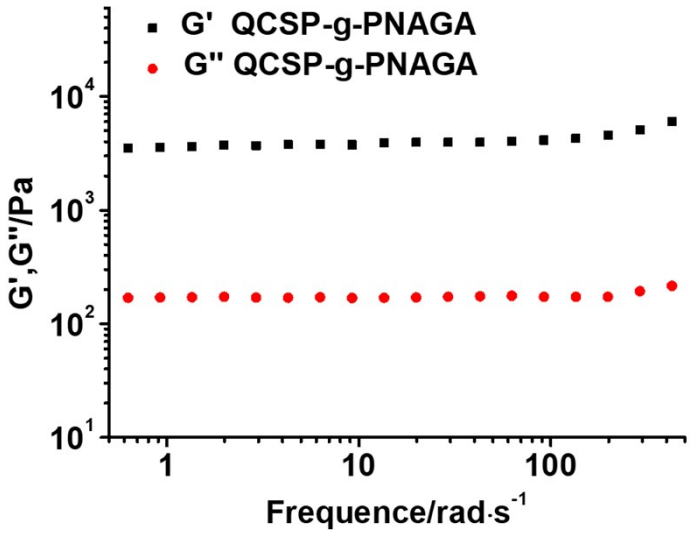

Fig. S10. The storage modulus (G′) and loss modulus (G″) of QCSP-g-PNAGA hydrogel tested in frequency sweep mode.

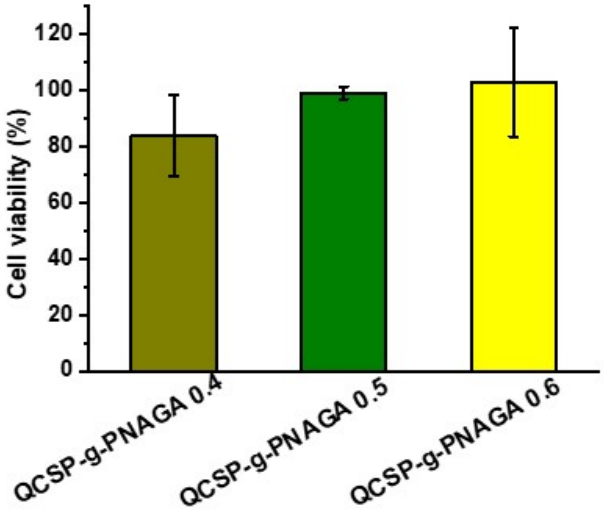

Fig. S11. Cell viability by MTT assay in the media with different hydrogels

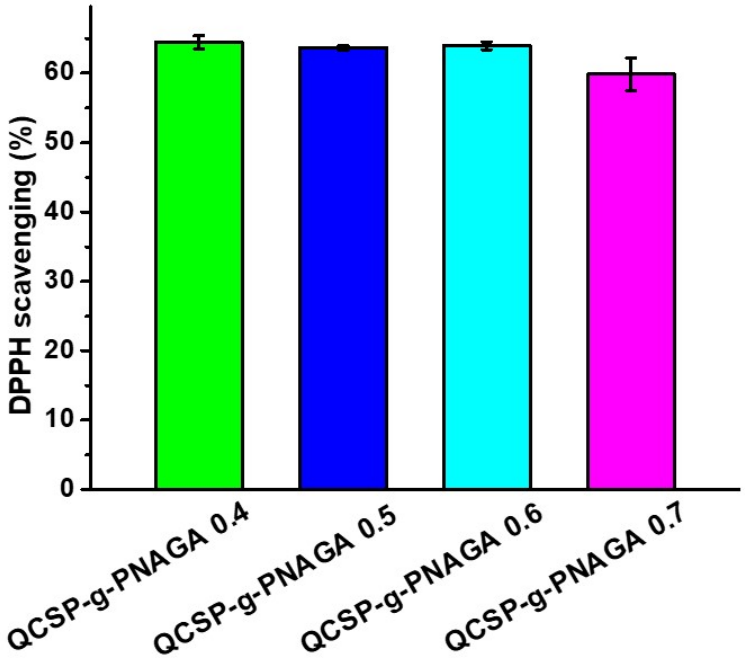

Fig. S12. DPPH scavenging efficiency of different hydrogels.

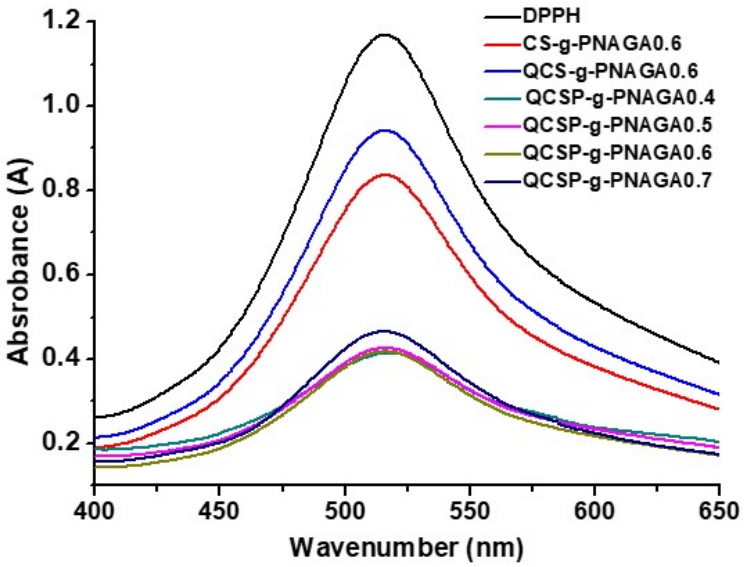

Fig. S13. UV−vis spectra of blank DPPH, CS-g-PNAGA-0.6, QCS-g-PNAGA-0.6, QCSP-g-PNAGA-0.4, QCSP-g-PNAGA-0.5, QCSP-g-PNAGA-0.6 and QCSP-g-PNAGA-0.7.

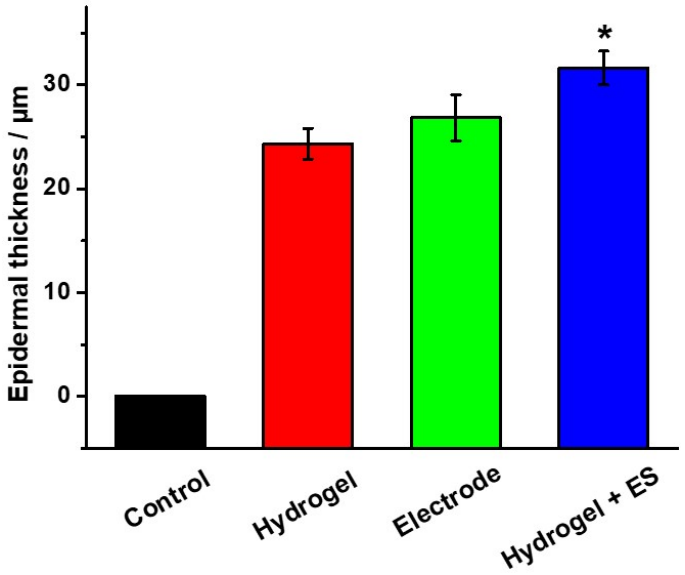

Fig. S14. Thickness of regenerated epidermal layers at the wound area on Day 14. * indicates significant difference comparing with the Control group .